MIT Open Access Articles

Response of the North Pacific Tropical Cyclone Climatology to Global Warming: Application of Dynamical Downscaling to CMIP5 Models

Massachusetts Institute of Technology

Response of the North Pacific Tropical Cyclone Climatology to Global Warming: Application of Dynamical Downscaling to CMIP5 Models

Lei Zhang

Cooperative Institute for Research in Environmental Sciences, University of Colorado Boulder, Boulder, Colorado

Kristopher B. Karnauskas

Cooperative Institute for Research in Environmental Sciences, and Department of Atmospheric and Oceanic Sciences, University of Colorado Boulder, Boulder, Colorado

Jeffrey P. Donnelly

Department of Geology and Geophysics, Woods Hole Oceanographic Institution, Woods Hole, Massachusetts

Kerry Emanuel

Program in Atmospheres, Oceans, and Climate, Department of Earth, Atmospheric, and Planetary Sciences, Massachusetts Institute of Technology, Cambridge, Massachusetts

ABSTRACT

A downscaling approach is applied to future projection simulations from four CMIP5 global climate models to investigate the response of the tropical cyclone (TC) climatology over the North Pacific basin to global warming. Under the influence of the anthropogenic rise in greenhouse gases, TC-track density, power dissipation, and TC genesis exhibit robust increasing trends over the North Pacific, especially over the central subtropical Pacific region. The increase in North Pacific TCs is primarily manifested as increases in the intense and relatively weak TCs. Examination of storm duration also reveals that TCs over the North Pacific have longer lifetimes under global warming.

Through a genesis potential index, the mechanistic contributions of various physical climate factors to the simulated change in TC genesis are explored. More frequent TC genesis under global warming is mostly attributable to the smaller vertical wind shear and greater potential intensity (primarily due to higher sea surface temperature). In contrast, the effect of the saturation deficit of the free troposphere tends to suppress TC genesis, and the change in large-scale vorticity plays a negligible role.

1. Introduction

The North Pacific is an important region of relatively frequent tropical cyclones (TCs) (~40 TCs per year). The extreme rainfall and strong winds associated with TCs may influence shipping in the open ocean and cause notable damage to coastal areas if TCs make landfall.

Given the possible catastrophic impact of TCs on mankind, the response of TC activity over the North Pacific basin to anthropogenic global warming is naturally of great societal interest and has been intensively analyzed in numerous studies (Zhao and Held 2012; Emanuel 2013; Murakami et al. 2013; Knutson et al. 2015; Kossin et al. 2016).

There are several approaches to investigating the relationship between climate change and TCs. One relatively straightforward approach is to analyze the future projections of TC statistics as explicitly resolved within the global model simulations. The current generation of climate models has indeed been suggested to be capable of simulating TCs (Zhao and Held 2010; Murakami et al.

ⓐ Denotes content that is immediately available upon publication as open access.

Corresponding author e-mail: Lei Zhang, lezh8230@colorado.edu

2013, 2015; Han et al. 2016). However, it has also been pointed out that the resolution of these models may be too coarse to properly resolve the full intensity spectrum of TCs, especially for intense storms (Emanuel 2006; Rotunno et al. 2009; Zhao et al. 2009). Therefore, the reliability of the projected changes in TC statistics in climate models remains questionable. Some studies use the statistical downscaling approach to examine future changes in TCs (e.g., Villarini and Vecchi 2012, 2013). Alternatively, several dynamical downscaling approaches have been developed, using high-resolution models embedded within global climate models (Knutson et al. 1998; Emanuel et al. 2008; Knutson et al. 2010; Emanuel 2010). Such techniques produce highly resolved TCs including a more realistic intensity spectrum. Also, because the high-resolution models are normally driven by the large-scale thermodynamic and dynamic conditions obtained from the global climate models or reanalysis datasets, results from downscaling models provide useful insights into the impacts of large-scale climate conditions on TC activity (Emanuel 2013). One limitation common to all applications of such a technique, however, is the lack of feedbacks between the simulated TCs and the global climate system. In general, if a strong TC exists, it is unfavorable for coexistence of other TCs in the same basin (Satoh et al. 2015), but such an effect is not included in most downscale techniques.

Downscaling approaches have been widely used to explore the response of TCs to global warming via the buildup of greenhouse gases (e.g., Emanuel et al. 2008; Villarini and Vecchi 2012; Knutson et al. 2013; Emanuel 2013). Using a regional model to downscale global climate models from phases 3 and 5 of the Coupled Model Intercomparison Project (CMIP3 and CMIP5), Knutson et al. (2013) found that over the North Atlantic basin, TCs become less frequent overall but shift toward more intense storms. In contrast, Villarini and Vecchi (2012) used a statistical model with sea surface temperature (SST) being the only predictor and found negligible changes in TC frequency over the North Atlantic during the twenty-first century. With a two-step downscaling framework, Knutson et al. (2015) found a decrease (increase) in TC frequency over the western (eastern) North Pacific in response to anthropogenic global warming. Emanuel et al. (2008) and Emanuel (2013) developed a novel dynamical downscaling technique and found increased TCs over both the North Atlantic and North Pacific basins. Kossin et al. (2016) used the same downscaling technique and found the same poleward shift of the average latitude where the TCs reach their lifetime maximum intensity over the western North Pacific as with observed tracks over the past 30 years. In this study, the downscaling technique of Emanuel et al.

(2008) is applied to four CMIP5 climate models to explore the response of the TCs over the North Pacific basin to global warming. In Emanuel (2013), future projection experiments under the representative concentration pathway (RCP) 8.5 emission scenario were analyzed, while in this study, both the RCP4.5 and RCP8.5 scenarios are analyzed to illustrate the response of TCs to both a moderate and relatively severe global warming scenarios. A further goal of this paper is to provide a better understanding of the physical mechanisms for projected changes of TCs under global warming through robust diagnostics.

As mentioned previously, none of the downscaling techniques allows tropical cyclones to feed back to the large-scale climate state. The technique used here predicts a general increase in the frequency of tropical cyclones, whereas most other dynamical downscaling techniques project decreasing frequency, as do global models that explicitly, albeit crudely, resolve tropical cyclones. The global models and most dynamical downscaling techniques fail to capture the high-intensity events that in practice are responsible for most damage and loss of life. While the technique used here captures the full spectrum of tropical cyclone intensity, it generates storms by random seeding and natural selection rather than as a natural consequence of the evolution of atmospheric features. While this random seeding captures the seasonal cycle and spatial variability of storms in the present climate, there is no guarantee that it accurately represents the response of TCs to global climate change. This caveat should be borne in mind in interpreting the results that follow.

Another set of studies of relevance to how TCs respond to climate change are "TC-world simulations" (Held and Zhao 2008; Khairoutdinov and Emanuel 2013), which examine storms that develop from horizontally homogeneous radiative–convective equilibrium states. These storms are back to back and form a fairly uniform array. As temperature increases, the storms become larger and their diameters appear to scale as the square root of the saturation mixing ratio (Khairoutdinov and Emanuel 2013). Thus, there are fewer storms per unit area. We do not, however, believe that these results are immediately applicable to the modern real world, in which the number of tropical cyclones does not appear to be limited by the packing density of such storms.

2. Models and methodology

The downscaling technique introduced in Emanuel et al. (2008) is applied to four CMIP5 models under the RCP4.5 and RCP8.5 emission scenarios over the period

TABLE 1. Four CMIP5 climate models used for the downscaling approach in this study.

Model	Modeling center (country)	AGCM resolution (longitude by latitude)	References
GFDL CM3	NOAA/Geophysical Fluid Dynamics Laboratory (United States)	$2.5° \times 2°$	Donner et al. (2011)
HadGEM2-ES	Met Office Hadley Centre (United Kingdom)	$1.875° \times 1.24°$	Collins et al. (2011)
IPSL-CM5A-LR	L'Institut Pierre-Simon Laplace (France)	$3.75° \times 1.875°$	Dufresne et al. (2013)
MIROC5	Atmosphere and Ocean Research Institute (The University of Tokyo), National Institute for Environmental Studies, and Japan Agency for Marine-Earth Science and Technology (Japan)	$1.40625° \times 1.40625°$	Watanabe et al. (2010)

2006–2100. In the RCP4.5 (RCP8.5) experiments, the radiative forcing reaches $4.5\,\mathrm{W\,m^{-2}}$ $(8.5\,\mathrm{W\,m^{-2}})$ in the year 2100. Global models included in this study are the NOAA/Geophysical Fluid Dynamics Laboratory Climate Model, version 3 (GFDL CM3); the Hadley Centre Global Environmental Model, version 2–Earth System (HadGEM2-ES); the L'Institut Pierre-Simon Laplace Coupled Model, version 5A, low resolution (IPSL-CM5A-LR); and the Model for Interdisciplinary Research on Climate, version 5 (MIROC5). Full references and some relevant details are provided in Table 1.

In the downscaling model, synthetic TCs are produced with a random seeding in space and time over the North Pacific basin. The TC tracks are then predicted by a beta-advection model driven by the large-scale winds from the climate models. Along each track, a deterministic model is used for intensity prediction. This is an axisymmetric atmospheric model phrased in angular-momentum coordinates and coupled to a one-dimensional ocean model. Thermodynamic and dynamic inputs to this intensity model are also obtained from climate models, including daily vertical wind shear between 250 and 850 hPa and monthly mean potential intensity, 600-hPa temperature, and specific humidity.

The intensity model predicts that most of the randomly placed seed vortices dissipate almost immediately, and these are discarded. The survivors are regarded as constituting the TC climatology of the downscaled model or reanalysis. Thus, the technique can be regarded as a form of natural selection. It has been shown in previous studies that this downscaling technique produces a realistic TC climatology (Emanuel 2006; Emanuel et al. 2008; Emanuel 2010).

One advantage of this technique is that thanks to a small run time, it is capable of generating a large number of synthetic TCs ($\sim 10^3$ per year), which keeps the random interannual variability of TC counts at less than 5%, and therefore provides useful insights into the dependence of TC activities on the given climate conditions (Emanuel 2013). Interested readers can refer to Emanuel et al. (2008) for a more in-depth description of this downscaling model.

3. Results

a. Downscaled response of TC climatology to global warming

Over the North Pacific basin, TCs propagate westward after genesis at low latitudes and retreat northward and eastward over mid- and high latitudes. As a result, the climatological TC-track density is centered over the subtropical North Pacific and midlatitude central Pacific to the east of Japan (Figs. 1a,b). Ensemble mean results from downscaling models suggest a robust and pronounced increasing trend in the TC-track density over most of the North Pacific region, with the maximum positive trend located over the central subtropical Pacific (Figs. 1a,b). Consistently, the power dissipation index (PDI), which is defined as the time integral of the cubed maximum surface wind speed along the TC track (Emanuel 2005), also exhibits a prominent increasing trend, especially over the subtropical region (Figs. 1c,d). Hence, TCs over the North Pacific clearly become more frequent in the RCP4.5 and RCP8.5 experiments; the increasing trends are more pronounced in the RCP8.5 case.

The domain-averaged TC-track density and PDI over the North Pacific basin indeed exhibit steadily increasing trends with noticeable interannual variability, and the intermodel spread increases with time during the period 2006–2100 (Figs. 2a,b). We note that the significant increasing trends of the TC-track density and the PDI influence some land areas with very high population density (e.g., Southeast Asia and North America) (Fig. 1). The population-density-weighted, North Pacific–averaged TC-track density and PDI exhibit significant increasing trends as well, albeit with larger intermodel spread (Figs. 2c,d). Hence, based on the results shown here, a large portion of the population would be affected by the more frequent TCs under global warming. Such a result is of important societal interest, given the catastrophic impacts of TCs.
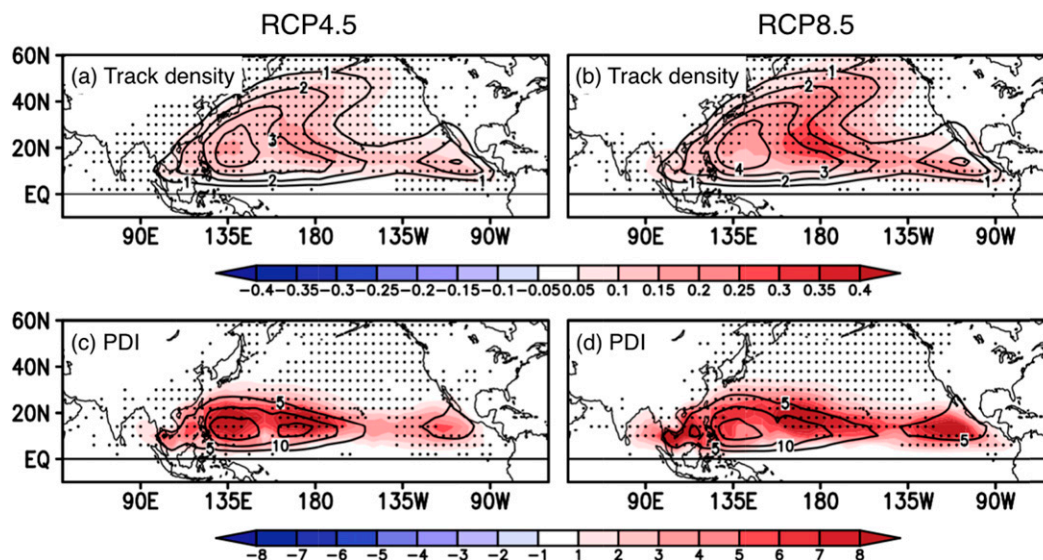
FIG. 1. Ensemble mean linear trend of the TC-track density (shading; number of tracks per decade) in the downscaling models for (a) RCP4.5 and (b) RCP8.5 experiments. Contours denote the climatological distribution of TC-track density over the period 2006–50. TC-track density is defined as the number of tracks in each $4° \times 4°$ grid per year. (c) RCP4.5 and (d) RCP8.5 show PDI trend (shading; $1.0 \times 10^8 \, \text{m}^3 \, \text{s}^{-2} \, \text{decade}^{-1}$) and climatology (contours; $1.0 \times 10^9 \, \text{m}^3 \, \text{s}^{-2}$). Stippling denotes the region where all the four models agree with the sign of the ensemble mean trend.

The changes of TC intensities are analyzed using a kernel probability density estimator. We find that the increasing trend in TC activity under global warming is primarily manifest as a greater frequency of both intense storms and relatively weak TCs, whereas the moderate TCs become less frequent (Figs. 3a–c). The well-developed TCs tend to become even more intense under global warming, which is likely due to the greater energy supply from the warmer sea surface (further diagnostics provided in section 3b). Note that the total number of TCs over the North Pacific basin increases during the twenty-first century in the downscaled experiments (Fig. 3d), which is consistent with the increase in the TC-track density over the North Pacific. In our downscaling model, changes in TC activity can be affected by two factors: changes in TC frequency and systematic migrations of TC tracks. As a result, the number of moderate TCs actually increases slightly because of the increase in the total TC number (figure not shown), despite the negative fractional change.

The probability density estimates for TC duration during the first and second half of the twenty-first century are also analyzed. The majority of TCs last around 4 to 12 days in the downscaling models (Fig. 4). More importantly, we find that during the second half of the twenty-first century, TCs tend to last longer compared to the first half of the century (Figs. 4a–c). The longer lifetime of TCs may be related to more favorable conditions for TCs in a warmer climate. In addition, the forward speed of TCs robustly becomes slower in response to anthropogenic global warming in the downscaling models (figure not shown), which also favors longer TC lifetimes. We also note that the fractional changes of TCs with different intensities and duration are more significant over the eastern Pacific than the western Pacific basin (Figs. 3 and 4) and slightly more evident in RCP8.5 than the RCP4.5 experiments (figure not shown).

b. TC genesis and GPI

Consistent with the positive trends of the TC-track density and the PDI over the North Pacific, TC genesis, which is defined as occurring when the TC's maximum surface wind speed first reaches $15 \, \text{m s}^{-1}$, also increases in the downscaled experiments (Figs. 5a,b), with a greater positive trend in RCP8.5 experiments compared to the RCP4.5 experiments. A genesis potential index (GPI) developed by Emanuel (2010) is employed here to explore the contributions of the various climate factors to the increase of TC genesis under global warming. This index is defined as follows:

$$\text{GPI} \equiv |\eta^3| \chi^{(-4/3)} \text{MAX}[(V_{\text{pot}} - 35 \, \text{m s}^{-1}), 0]^2$$
$$\times (25 \, \text{m s}^{-1} + V_{\text{shear}})^{-4}, \qquad (1)$$
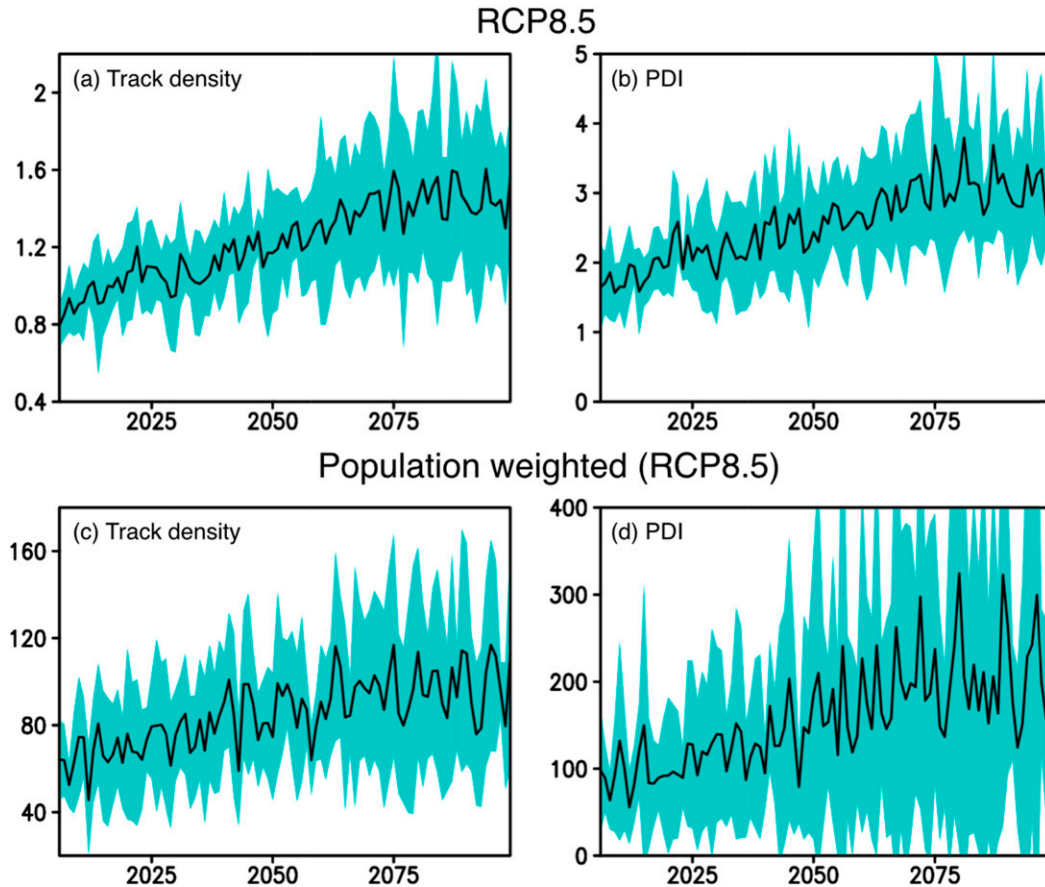
FIG. 2. Time series of the ensemble mean domain-averaged (a) TC-track density and (b) PDI ($1.0 \times 10^9 \, \text{m}^3 \, \text{s}^{-2}$) over the North Pacific basin (0°–60°N, 60°E–60°W). Shading denotes one standard deviation across the four downscaling CMIP5 models. (c),(d) Population-density-weighted results. Units are 1.0×10^9 person $\text{m}^3 \, \text{s}^{-2} \, \text{km}^{-2}$ for the PDI. (Population density data are available at http://sedac.ciesin.columbia.edu/data/collection/gpw-v3.)

in which η is the absolute vorticity of the 850-hPa flow, V_{pot} the potential intensity, and V_{shear} the magnitude of the vertical wind shear between 850 and 250 hPa. The term χ is a nondimensional parameter defined in Emanuel (1995):

$$\chi = \frac{h^* - h_m}{h_0^* - h^*}, \tag{2}$$

where h^* represents the saturation moist static energy of the free troposphere, h_0^* the saturation moist static energy at the surface, and h_m the actual moist static energy of the midtroposphere. At fixed relative humidity, the numerator increases with temperature at a rate of around 6%~7% K^{-1}, following the Clausius–Clapeyron relationship. The denominator, on the other hand, increases in proportion to the surface turbulent enthalpy flux, which is constrained by the net radiative cooling of the troposphere in the global mean sense and thus increases at a much slower rate

under global warming (Vecchi and Soden 2007). As a result, one may expect an increase in the global mean χ due to global warming, which would contribute to a decrease in GPI based on Eq. (1) and thus is unfavorable for TC genesis. Note that the increase of χ essentially reflects the effect of the saturation deficit of the free troposphere on TC genesis under global warming.

Changes in GPI and TC genesis agree very well in the downscaling model; the GPI increases over the North Pacific, especially over the subtropical central and eastern Pacific, where a large positive trend of TC genesis is located (Fig. 5). To the east of the Philippines, where TC genesis exhibits a negligible trend, the GPI trend is also small or even negative (Figs. 5c,d). Hence, it is clear that the GPI method is a useful diagnostic of TC genesis. To explore the effects of climate conditions on the increasing trend of the GPI, linear trends of the various climate factors that are incorporated into the GPI are analyzed (Fig. 6).
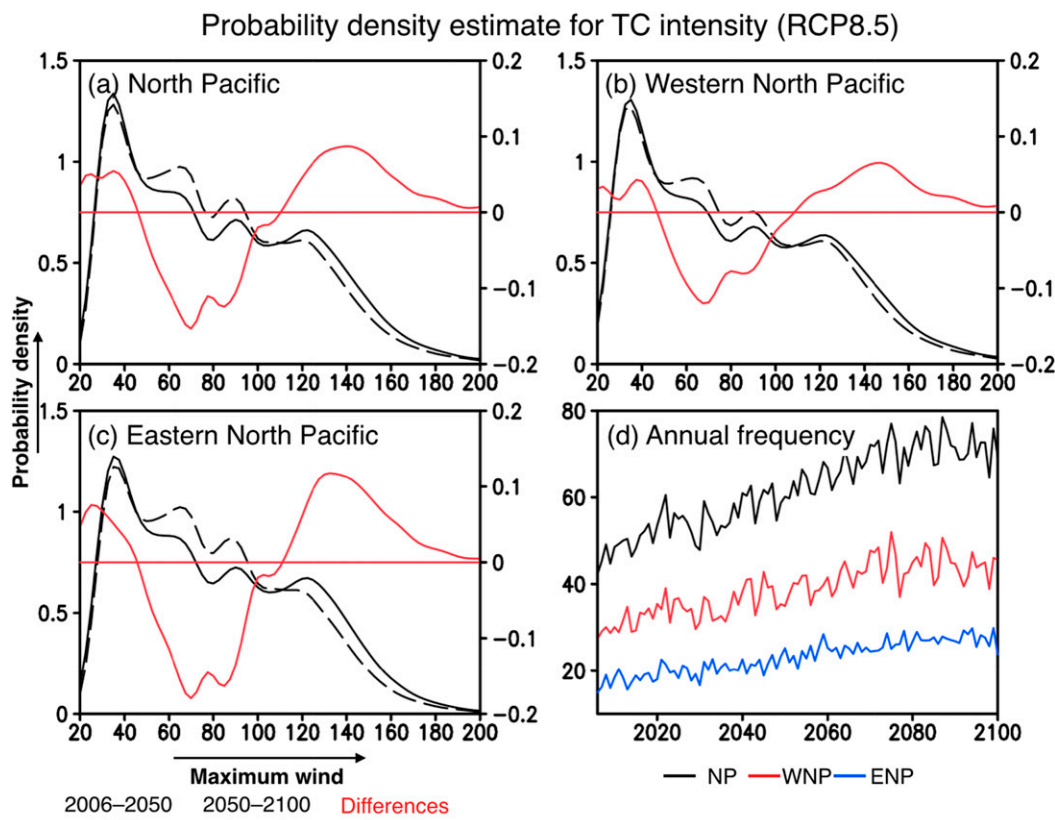
FIG. 3. Probability density estimate for TC intensity (measured in knots) in RCP8.5 experiments. Results are shown for the (a) North Pacific basin, (b) for the western North Pacific, and (c) for the eastern North Pacific. Black solid (dashed) line for the result over the period 2050–2100 (2006–50) (left axis; unit is %). Red for the difference between the two time periods (right axis; unit is %). (d) TC frequency during 2006–2100. Black line denotes the result for the entire North Pacific and blue (red) for the eastern (western) North Pacific.

Vertical wind shear is projected to be weakening nearly ubiquitously over the North Pacific, especially over the subtropical region, which favors the TC genesis (Fig. 6a). Such a result is consistent with Held and Soden (2006), who found weakening of the atmospheric overturning circulation in future projections from climate models, which is further related to the greater rate of moisture increase compared to that of rainfall under global warming. A positive trend of the large-scale vorticity is found over the midlatitude North Pacific, away from the primary TC genesis region (Fig. 6b). We note that a negative trend of the low-level vorticity appears over the eastern Pacific, accompanied by stronger vertical wind shear (Figs. 6a,b). Such changes might be attributable to the widening of the Hadley cell and intensification of the intertropical convergence zone (ITCZ) over the eastern Pacific under global warming (e.g., Hu and Fu 2007; Lu et al. 2007; Lau et al. 2013; Zhang and Li 2016), which thereby leads to stronger vertical wind shear, strengthened descending motion, and low-level anticyclonic anomalies over the

subtropical eastern Pacific, which tend to suppress the TC genesis. The potential intensity exhibits a nearly ubiquitous positive trend, which contributes to the increase in the GPI and is thus favorable for the TC genesis (Fig. 6c). Such change is primarily attributable to the nearly ubiquitous surface warming in the future projections from CMIP5 models. The parameter χ also increases over most regions, as expected, and therefore the saturation deficit effect indeed acts against the positive trend in the GPI (Fig. 6d). Note that the models agree well on the PI trends compared to other factors of the GPI, which may be because of relatively better agreement of predicted SST trends across different models, which project strongly onto PI, whereas the atmospheric metrics are less robust.

The differences between the RCP4.5 and RCP8.5 experiments are consistent with the aforementioned conclusions; that is, a more severe warming scenario induces smaller vertical wind shear and greater potential intensity that contribute to the positive trend in the GPI, whereas the more pronounced saturation deficit effect
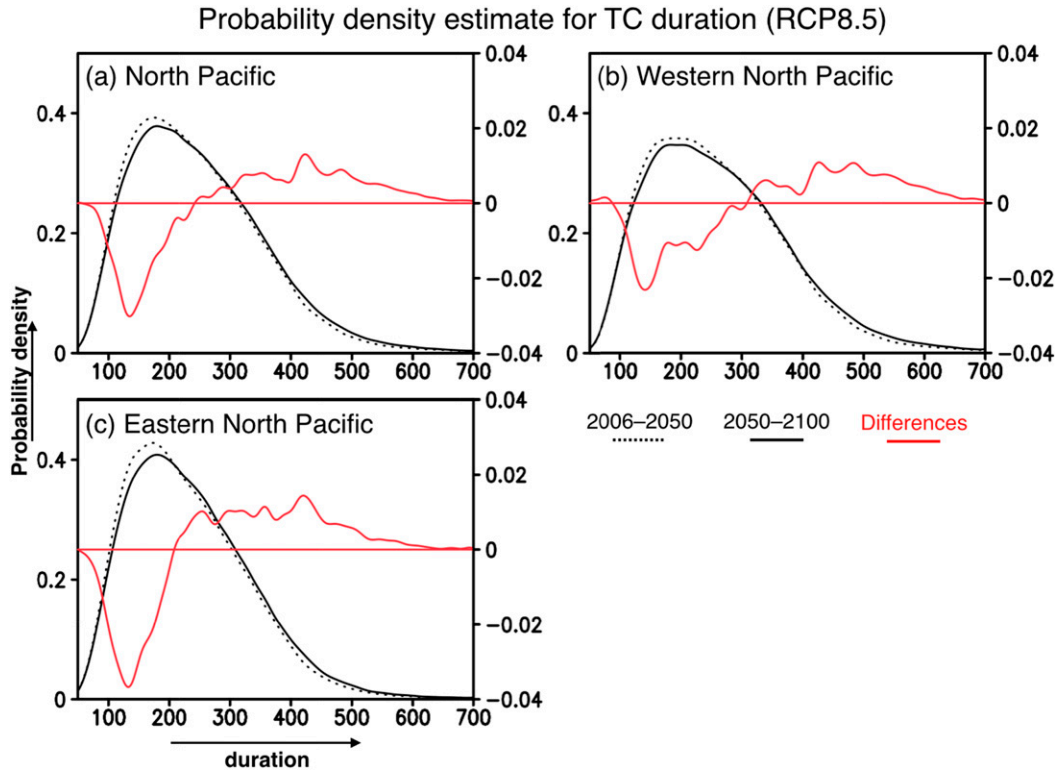
FIG. 4. As in Fig. 3, but for the probability density estimate of TC duration (hour).

tends to decrease the GPI (Fig. 7). The large-scale vorticity trend is positive over the midlatitude North Pacific and negative over the subtropical eastern Pacific, with a stronger vertical wind shear. Note that the potential intensity is the only factor that contributes to the increase in the GPI over the eastern Pacific (Figs. 5, 6c, and 7c), where the largest positive trend of the potential intensity is located. This result is likely related to the
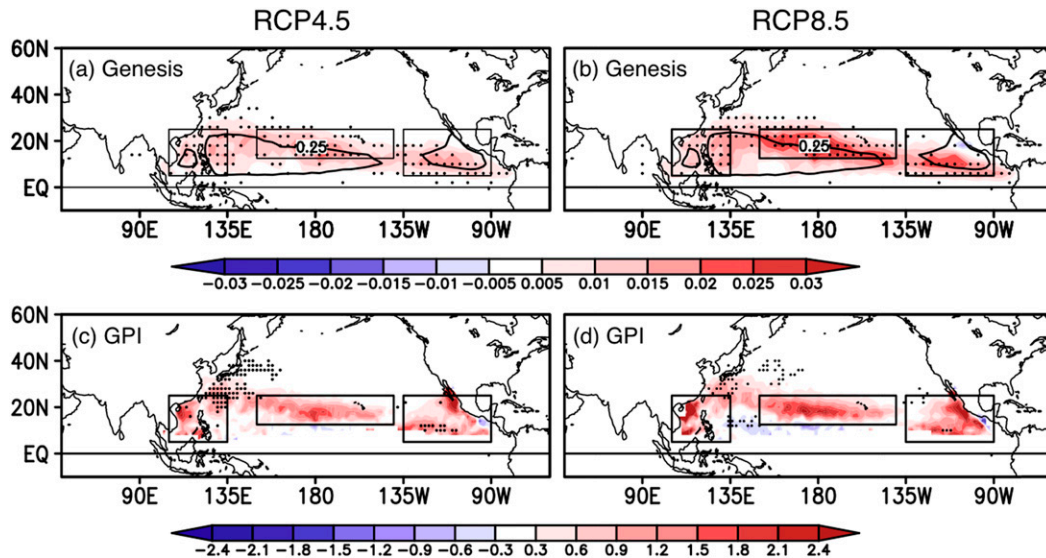

FIG. 5. As in Fig. 1, but for (a),(b) TC genesis and (c),(d) the GPI. TC genesis is defined as the first grid in which the maximum surface wind speed of the TC reaches $15 \, \text{m s}^{-1}$. Boxes denote the regions where the positive trends in TC genesis and the GPI are significant.
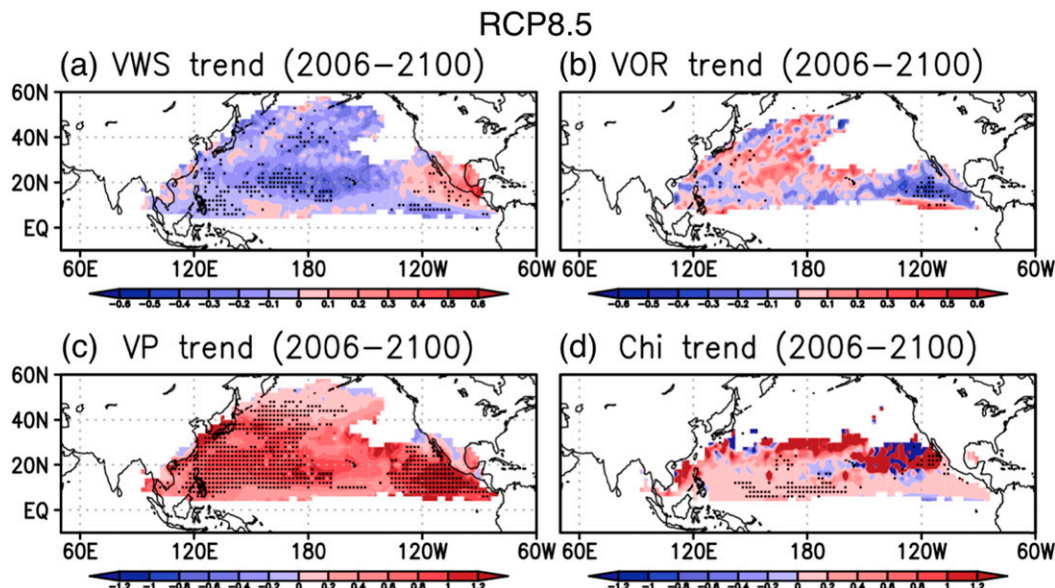
FIG. 6. Ensemble mean linear trends of (a) vertical wind shear (m s^{-1} decade^{-1}), (b) absolute vorticity of the 850-hPa flow (1.0×10^{-6} s^{-1} decade^{-1}), (c) the potential intensity (m s^{-1} decade^{-1}), and (d) χ (1.0×10^{-1} decade^{-1}) over the period 2006–2100 in RCP8.5 downscaling experiments. Stippling denotes the region where all the four models agree with the sign of the ensemble mean trend.

pronounced eastern Pacific SST warming that most CMIP5 models simulate (e.g., Vecchi and Soden 2007; Xie et al. 2010).

Finally, the relative contributions of the trend in each climatic variable represented by the GPI trend are explored by linearizing Eq. (1) through the natural logarithm of the full equation. Using this approach for the North Pacific basin, we find that the largest and most robust increase in log(GPI) is located over the central Pacific, which is primarily attributable to the effects of greater potential intensity and smaller vertical wind shear (Fig. 8). The saturation deficit effect tends to
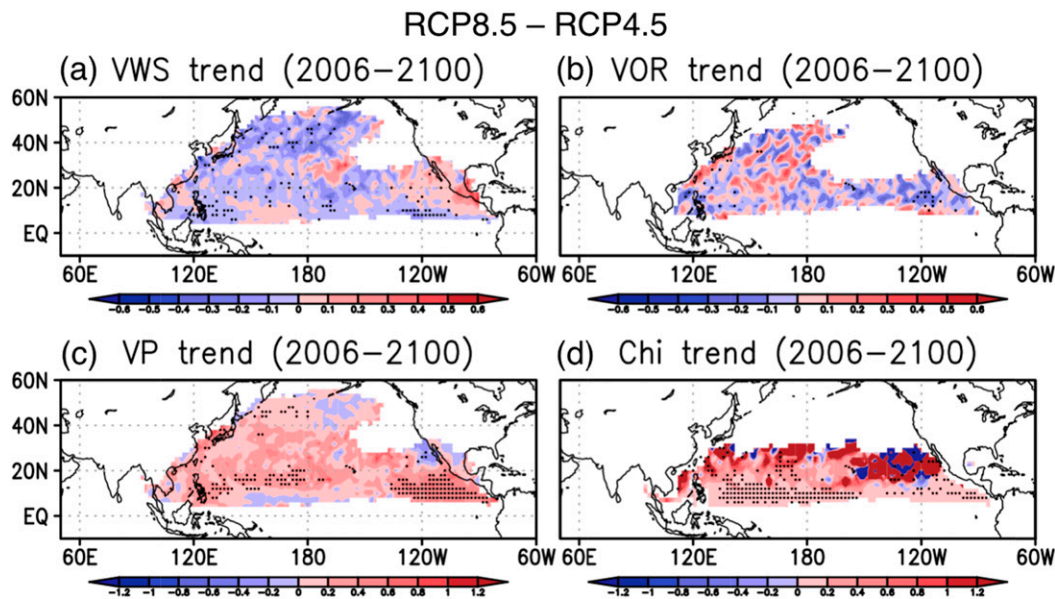

FIG. 7. As in Fig. 6, but for the differences between the RCP4.5 and RCP8.5 downscaling experiments (RCP8.5 minus RCP4.5).
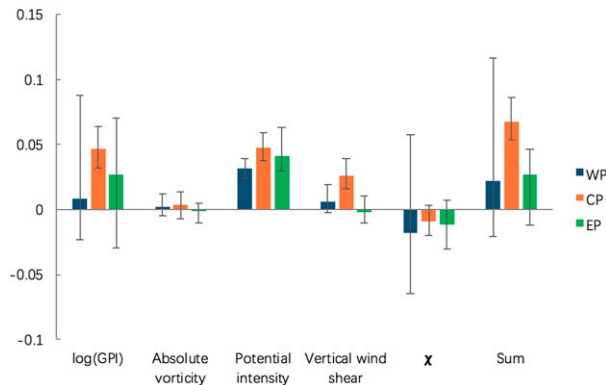
FIG. 8. Domain-averaged linear trends of log(GPI) per decade and the various climate factors that contribute to the changes of log(GPI) in the RCP8.5 experiments, including absolute vorticity of the 850-hPa flow, potential intensity, vertical wind shear, and χ. The sum of the four factors is also shown. Vertical error bar denotes the largest and smallest values from the four models analyzed in this study: blue for the western Pacific region (5°–25°N and 105°–135°E), orange for the central Pacific (12.5°–25°N and 150°E–140°W), and green for the eastern Pacific (5°–25°N and 135°–90°W). Domains are marked in Fig. 5.

suppress TC genesis, and the change in the large-scale vorticity plays a negligible role. Over the western and eastern North Pacific, the positive GPI trend is smaller and less certain compared to the central Pacific region, and the increase of the GPI is mainly induced by greater potential intensity, which is partly offset by the effect of the positive trend in χ. The effects of changes in the vertical wind shear and large-scale vorticity are insignificant (Fig. 8). We note that the increasing trends in TC-track density and PDI begin to level off after around the year 2070 (Fig. 2), despite the radiative forcing continuing increasing beyond 2070 in RCP8.5 experiments, which is related to a more prominent saturation deficit effect of free troposphere during the late twenty-first century (figure not shown).

4. Summary and conclusions

Applying a downscaling approach to future projection experiments from four CMIP5 climate models, we quantify and diagnose the response of the TC climatology over the North Pacific basin to global warming. We find that under global warming, the TC-track density and PDI both exhibit robust and pronounced increasing trends over the North Pacific basin, especially over the central subtropical Pacific, and the positive trends are more significant in the RCP8.5 experiments than in the RCP4.5 experiments. The increase in North Pacific TCs is primarily manifest as increases in both the intense and the relatively weak TCs, whereas the number of moderate TCs only increases slightly. Developed TCs over the North Pacific also tend to last longer in a warmer climate.

Consistent with the more frequent TCs over the North Pacific under global warming, TC genesis also exhibits a positive trend over the subtropical North Pacific. Decomposition of the GPI reveals that the increasing trend in TC genesis is primarily attributable to the smaller vertical wind shear and greater potential intensity (higher SST), whereas the saturation deficit effect χ tends to suppress the TC genesis. The large-scale low-level vorticity change plays a negligible role in the GPI trend. We note that the changes in both the vertical wind shear and χ can be explained by the moisture–rainfall mismatch (i.e., the slower increasing rate of precipitation relative to atmospheric moisture content), and the two opposite effects tend to partly offset each other.

Our results suggest that the future may bear more frequent and intense TCs over the North Pacific, which may create a substantial impact on Southeast Asia, the Pacific islands, and North America, where the population density is large. Our result is different from Knutson et al. (2015), who found overall decreased TC frequency but more frequent intense storms over the western North Pacific in response to the anthropogenic global warming. Over the eastern North Pacific, on the other hand, our finding is consistent with the results from Knutson et al.'s (2015) study (i.e., more frequent TCs and intense storms under global warming). In addition to different downscaling approaches, we note that the subset of CMIP5 models used in Knutson et al.'s (2015) study is also different from those in this study.

The downscaling approach employed in this study essentially reflects the response of the TCs to the projected changes of the climate conditions in climate models in response to the anthropogenic rise in greenhouse gases. However, the simulated changes of the various climate factors are uncertain across different climate models and compared to the observations to some extent. For instance, the large increasing trend in potential intensity plays an important role in the increase of TC genesis over the eastern Pacific, which is likely related to the pronounced eastern Pacific SST warming that climate models tend to simulate; the observed change to date in zonal SST gradient, on the other hand, is negligible or even slightly enhanced during the twentieth century (Karnauskas et al. 2009; Zhang 2016). Such discrepancies represent one potential source of uncertainty in the results.

Given the considerable stakes, further efforts should strive to understand the differences in the results given by various approaches to quantifying the response of

TCs to anthropogenic climate change. A TC downscaling model intercomparison project is needed for such a purpose, the idea of which is similar to the tropical cyclone climate model intercomparison project (TC-MIP) in Walsh et al. (2010) but for downscaling results using the same subset of CMIP5 models.

REFERENCES

Collins, W., and Coauthors, 2011: Development and evaluation of an Earth-system model—HadGEM2. *Geosci. Model Dev.*, **4**, 1051–1075, doi:10.5194/gmd-4-1051-2011.

Donner, L. J., and Coauthors, 2011: The dynamical core, physical parameterizations, and basic simulation characteristics of the atmospheric component AM3 of the GFDL Global Coupled Model CM3. *J. Climate*, **24**, 3484–3519, doi:10.1175/2011JCLI3955.1.

Dufresne, J.-L., and Coauthors, 2013: Climate change projections using the IPSL-CM5 Earth System Model: from CMIP3 to CMIP5. *Climate Dyn.*, **40**, 2123–2165, doi:10.1007/s00382-012-1636-1.

Emanuel, K., 1995: The behavior of a simple hurricane model using a convective scheme based on subcloud-layer entropy equilibrium. *J. Atmos. Sci.*, **52**, 3960–3968, doi:10.1175/1520-0469(1995)052<3960:TBOASH>2.0.CO;2.

——, 2005: Increasing destructiveness of tropical cyclones over the past 30 years. *Nature*, **436**, 686–688, doi:10.1038/nature03906.

——, 2006: Climate and tropical cyclone activity: A new model downscaling approach. *J. Climate*, **19**, 4797–4802, doi:10.1175/JCLI3908.1.

——, 2010: Tropical cyclone activity downscaled from NOAA-CIRES reanalysis, 1908–1958. *J. Adv. Model. Earth Syst.*, **2**, 1, doi:10.3894/JAMES.2010.2.1.

——, 2013: Downscaling CMIP5 climate models shows increased tropical cyclone activity over the 21st century. *Proc. Natl. Acad. Sci. USA*, **110**, 12 219–12 224, doi:10.1073/pnas.1301293110.

——, R. Sundararajan, and J. Williams, 2008: Hurricanes and global warming: Results from downscaling IPCC AR4 simulations. *Bull. Amer. Meteor. Soc.*, **89**, 347–367, doi:10.1175/BAMS-89-3-347.

Han, R., and Coauthors, 2016: An assessment of multimodel simulations for the variability of western North Pacific tropical cyclones and its association with ENSO. *J. Climate*, **29**, 6401–6423, doi:10.1175/JCLI-D-15-0720.1.

Held, I. M., and B. J. Soden, 2006: Robust responses of the hydrological cycle to global warming. *J. Climate*, **19**, 5686–5699, doi:10.1175/JCLI3990.1.

——, and M. Zhao, 2008: Horizontally homogeneous rotating radiative–convective equilibria at GCM resolution. *J. Atmos. Sci.*, **65**, 2003–2013, doi:10.1175/2007JAS2604.1.

Hu, Y., and Q. Fu, 2007: Observed poleward expansion of the Hadley circulation since 1979. *Atmos. Chem. Phys.*, **7**, 5229–5236, doi:10.5194/acp-7-5229-2007.

Karnauskas, K. B., R. Seager, A. Kaplan, Y. Kushnir, and M. A. Cane, 2009: Observed strengthening of the zonal sea surface temperature gradient across the equatorial Pacific Ocean. *J. Climate*, **22**, 4316–4321, doi:10.1175/2009JCLI2936.1.

Khairoutdinov, M. F., and K. Emanuel, 2013: Rotating radiative-convective equilibrium simulated by a cloud-resolving model. *J. Adv. Model. Earth Syst.*, **5**, 816–825, doi:10.1002/2013MS000253.

Knutson, T. R., R. E. Tuleya, and Y. Kurihara, 1998: Simulated increase of hurricane intensities in a CO_2-warmed climate. *Science*, **279**, 1018–1021, doi:10.1126/science.279.5353.1018.

——, and Coauthors, 2010: Tropical cyclones and climate change. *Nat. Geosci.*, **3**, 157–163, doi:10.1038/ngeo779.

——, and Coauthors, 2013: Dynamical downscaling projections of twenty-first-century Atlantic hurricane activity: CMIP3 and CMIP5 model-based scenarios. *J. Climate*, **26**, 6591–6617, doi:10.1175/JCLI-D-12-00539.1.

——, J. Sirutis, M. Zhao, R. Tuleya, M. Bender, G. Vecchi, G. Villarini, and D. Chavas, 2015: Global projections of intense tropical cyclone activity for the late twenty-first century from dynamical downscaling of CMIP5/RCP4.5 scenarios. *J. Climate*, **28**, 7203–7224, doi:10.1175/JCLI-D-15-0129.1.

Kossin, J. P., K. A. Emanuel, and S. J. Camargo, 2016: Past and projected changes in western North Pacific tropical cyclone exposure. *J. Climate*, **29**, 5725–5739, doi:10.1175/JCLI-D-16-0076.1.

Lau, K. M., H. T. Wu, and K. M. Kim, 2013: A canonical response of precipitation characteristics to global warming from CMIP5 models. *Geophys. Res. Lett.*, **40**, 3163–3169, doi:10.1002/grl.50420.

Lu, J., G. A. Vecchi, and T. Reichler, 2007: Expansion of the Hadley cell under global warming. *Geophys. Res. Lett.*, **34**, L06805, doi:10.1029/2006GL028443.

Murakami, H., B. Wang, T. Li, and A. Kitoh, 2013: Projected increase in tropical cyclones near Hawaii. *Nat. Climate Change*, **3**, 749–754, doi:10.1038/nclimate1890.

——, and Coauthors, 2015: Simulation and prediction of category 4 and 5 hurricanes in the high-resolution GFDL HiFLOR coupled climate model. *J. Climate*, **28**, 9058–9079, doi:10.1175/JCLI-D-15-0216.1.

Rotunno, R., Y. Chen, W. Wang, C. Davis, J. Dudhia, and G. J. Holland, 2009: Large-eddy simulation of an idealized tropical cyclone. *Bull. Amer. Meteor. Soc.*, **90**, 1783–1788, doi:10.1175/2009BAMS2884.1.

Satoh, M., Y. Yamada, M. Sugi, C. Kodama, and A. T. Noda, 2015: Constraint on future change in global frequency of tropical cyclones due to global warming. *J. Meteor. Soc. Japan*, **93**, 489–500, doi:10.2151/jmsj.2015-025.

Vecchi, G. A., and B. J. Soden, 2007: Global warming and the weakening of the tropical circulation. *J. Climate*, **20**, 4316–4340, doi:10.1175/JCLI4258.1.

Villarini, G., and G. A. Vecchi, 2012: Twenty-first-century projections of North Atlantic tropical storms from CMIP5 models. *Nat. Climate Change*, **2**, 604–607, doi:10.1038/nclimate1530.

——, and ——, 2013: Projected increases in North Atlantic tropical cyclone intensity from CMIP5 models. *J. Climate*, **26**, 3231–3240, doi:10.1175/JCLI-D-12-00441.1.

Walsh, K., S. Lavender, H. Murakami, E. Scoccimarro, L. P. Caron, and M. Ghantous, 2010: The tropical cyclone climate model intercomparison project. *Hurricanes and Climate Change*, J. Elsner et al., Eds., Springer, 1–24.

Watanabe, M., and Coauthors, 2010: Improved climate simulation by MIROC5: Mean states, variability, and climate sensitivity. *J. Climate*, **23**, 6312–6335, doi:10.1175/2010JCLI3679.1.

Xie, S. P., C. Deser, G. A. Vecchi, J. Ma, H. Teng, and A. T. Wittenberg, 2010: Global warming pattern formation: Sea surface temperature and rainfall. *J. Climate*, **23**, 966–986, doi:10.1175/2009JCLI3329.1.

Zhang, L., 2016: The roles of external forcing and natural variability in global warming hiatuses. *Climate Dyn.*, **47**, 3157–3169, doi:10.1007/s00382-016-3018-6.

——, and T. Li, 2016: Relative roles of anthropogenic aerosols and greenhouse gases in land and oceanic monsoon changes during past 156 years in CMIP5 models. *Geophys. Res. Lett.*, **43**, 5295–5301, doi:10.1002/2016GL069282.

Zhao, M., and I. M. Held, 2010: An analysis of the effect of global warming on the intensity of Atlantic hurricanes using a GCM with statistical refinement. *J. Climate*, **23**, 6382–6393, doi:10.1175/2010JCLI3837.1.

——, and ——, 2012: TC-permitting GCM simulations of hurricane frequency response to sea surface temperature anomalies projected for the late-twenty-first century. *J. Climate*, **25**, 2995–3009, doi:10.1175/JCLI-D-11-00313.1.

——, ——, S. J. Lin, and G. A. Vecchi, 2009: Simulations of global hurricane climatology, interannual variability, and response to global warming using a 50-km resolution GCM. *J. Climate*, **22**, 6653–6678, doi:10.1175/2009JCLI3049.1.